The Regional Geochemical Sampling Programme of Namibia (RGSP): Evaluating pXRF Results from Area 2116 Okahandja

Badumisa Sibolile*, Wilka Embula, Ute Schreiber, Gavine Kavindikiza and Ulf Kasuto

Geological Survey of Namibia, 6 Aviation Road, Windhoek
*Corresponding author: <Badumisa.Sibolile@mme.gov.na>

Abstract: - Systematic geochemical soil and stream sediment sampling by the Geological Survey of Namibia (GSN) commenced in 1999. The Regional Geochemical Sampling Programme follows the Final Report of the IGCP (International Geological Correlation Programme) Project 259. Its aim is to establish a National Baseline Geochemical Database of elements in the anthropogenically undisturbed geosphere. Baseline geochemical surveys have applications in mineral exploration, land use planning, agriculture, medical geology, and many other fields. 2850 stream sediment and soil samples, including 159 duplicates, were collected at pre-selected locations in the area covered by 250 k map sheet 2116 Okahandja. Preliminary geochemical data were obtained by analysing the fine fraction (<180 μm) by portable XRF (Niton Energy Dispersive XRF) at the GSN laboratory to assess the effectiveness of this method in regional surveys. Spatial distribution maps for Cu and Fe in soil and stream sediments were compiled with ESRI ArcGIS software, and interpreted in terms of underlying country rock and morphology.

Introduction

The Geological Survey of Namibia has been conducting a nationwide regional geochemical mapping programme for over two decades, starting in 1999. The purpose of the project is to develop a geochemical database of most elements in the geosphere, untampered by human activities, although much of the ground is farming land. To date, sampling of eight and a half 1:250 000 map sheets has been completed (Fig. 1), with over 21 000 samples collected in an area covering approximately 170 000 km^2 or slightly more than 20% of the country. The Okahandja map sheet, located in central Namibia, north of the capital Windhoek, was sampled in 2003/4. A total of 2850 samples was collected, with an average sample density of approximately one sample per 7-8 km^2. The analytical data of these samples will be useful across many sectors, such as land use planning, mineral exploration, medical geology, agriculture and environmental monitoring. The purpose of this report is to establish a method of presentation of the data obtained, as well as to evaluate the usefulness of pXRF in regional geochemical surveys intended to produce baseline data. Of the 43 elements analysed (Ag, Al, As, Au, Ba, Bi, Ca, Cd, Cl, Co, Cr, Cs, Cu, Fe (tot), Hf, Hg, K, Mg, Mn, Mo, Nb, Ni, P, Pb, Pd, Rb, Re, S, Sb, Sc, Se, Si, Sn, Sr, Ta, Te, Th, Ti, U, V, W, Zn, Zr), copper and iron were selected as test cases because of their comparative abundance, and relatively low minimum detection limits of ± 20 ppm and 50 ppm, respectively, on the analytical instrument chosen.

Topography and Survey Design

Area 2116 Okahandja encompasses some highly variable terrain. Altitudes between 1600 m and 1800 m are being attained in the south-eastern part, while isolated inselbergs rise several hundred metres above the surrounding plains in the west. The lowest elevations are recorded in the south-west (<1200 m) and north-east (<1400 m), where the terrain drops off to the Namib Plains and the Kalahari Sandveld, respectively. The greatest topographic prominences are Omatako (2286 m), followed by Otjihaena (2108 m) and Mt. Etjo (2082 m) in the north-western sector. The map area is drained by the ephemeral Swakop, Khan

and Omaruru Rivers, which flow westwards to the Atlantic coast, and their tributaries. The Omatako River rises in the Omatako Mountains and drains towards the Kalahari. All water-courses within the area flow only for short peri-

ods during a good rainy season, but – excluding exceptionally dry seasons - contain subsurface water at shallow depths throughout the year (Linus and Schreiber, 2017).
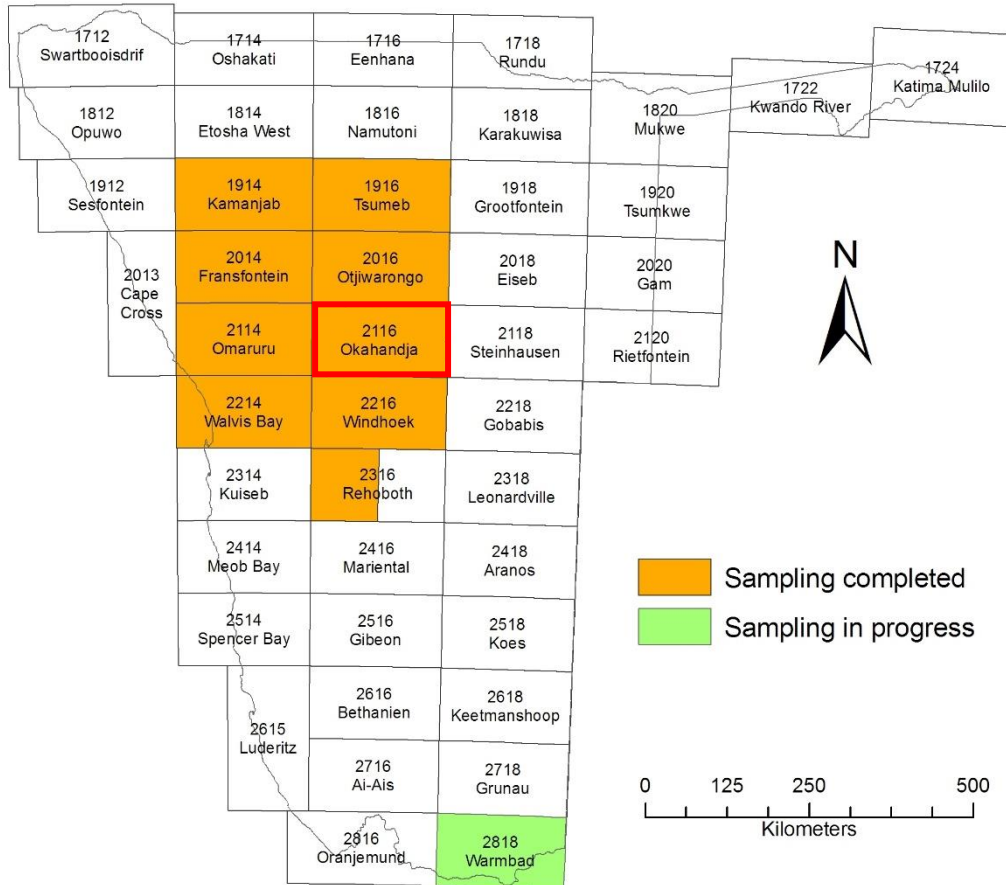

Figure 1. Index of 250 k map sheets showing the current status of the Regional Geochemical Sampling Programme (RGSP), with eight and a half sheets completed and one more in progress; area 2116 Okahandja is marked by the red box.

In the western, hilly part of the area (2116; Fig. 2) the drainage system is well-developed, and samples were taken mostly from second and third order streams, with a few from main drainage channels (i. e. Khan, Omaruru, Swakop, Omatako Omuramba) as control samples, and to detect potential anomalous values missed. Stream sediment sample locations were selected with the aim to cover drainage areas of approximately 10 km^2 or less per sample. Soil samples were taken to infill areas between drainages in the western part, while in the flat-lying east of the map area (area 2117; Fig. 2), where drainage channels are poorly developed or absent, soil samples predominate at a spacing of roughly one sample per 10 km^2.

While most stream sediment samples (except those within main drainages) were se-

lected to detect the geochemical composition of areas drained by small seasonally flowing streams, the soil samples reflect *in situ* weathering and leaching of the underlying bedrock. However, where the Kalahari overburden exceeds 10 m in the north-eastern sector of the map sheet (Fig. 2), little expression of the buried rocks can be expected to show in surface samples, as is borne out by the analytical results (Figs 9, 13).

Altogether 2691 locations were sampled within the survey area. Of these 1492 were from stream sediments or drainages (~55.5%), which constituted the preferred sample medium, as being representative of a larger terrain, while 1199 were soil samples (44.5%). In the western half of the map sheet (area 2116) the proportion of drainage to soil samples was 1272 : 220 (ex-

cluding duplicates), while in the east (area 2117), where drainages are less well defined and often barely distinguishable from the surrounding soil cover, soil samples dominate over drainage samples 762 : 437 (excluding duplicates), the latter taken mostly from the south-

western part (area 2117C; Fig. 2). For this reason, interpretation and visualisation of the analytical results is based on stream sediment samples in the western half of the area, and on soil samples in the east.
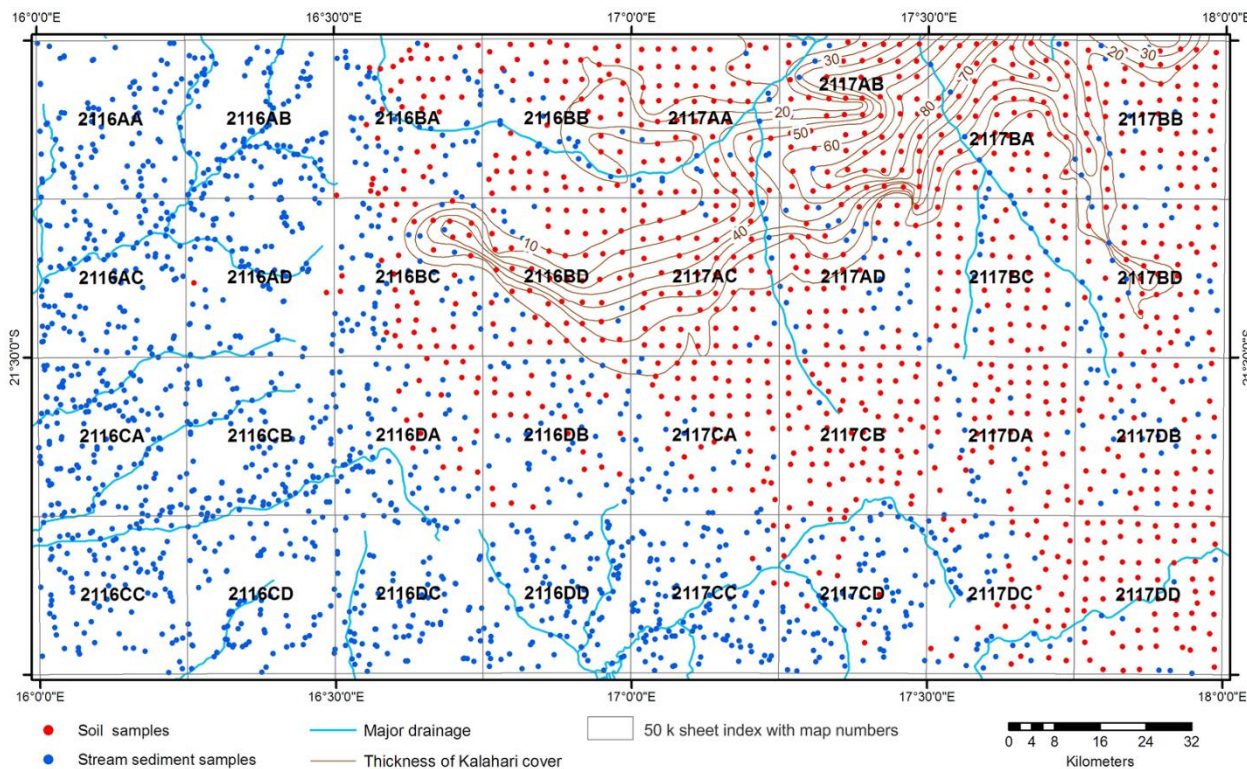

Figure 2. Survey layout showing positions of soil and stream sediment samples, major drainages and Kalahari isopachs

Sampling method

The RGSP is based largely on the recommendations of IGCP Project 259, also known as the "Blue Book", which outlines sampling protocols, sample handling, storage, analytical requirements and techniques for geochemical mapping in various environments. At each preselected sample location identified during the planning phase, five sample pits of ca. 25-30 cm depth were dug, and a composite sample obtained and screened. Two samples were collected, i. e. a coarse (<2 mm fraction) sample was placed in a 5 kg polystyrene bag, and a fine (<180 micron fraction) sample was stored in a 60 g polystyrene bag (Fig. 3). To avoid contamination, only wooden and plastic tools were used to collect and screen the samples. New gloves were used at each site to be worn during the major sampling stages, and the screening

Figure 3. Sample collection from a drainage channel showing the two size fractions collected

mesh was decontaminated by passing material from each new site before processing the actual sample. The samples were then riffle split and homogenised to obtain portions for analysis and archiving. All samples are stored at the GSN facilities in Windhoek.

Sample Preparation and Analysis

Geochemical analysis of the samples from the Okahandja area was focused on the fine fraction (<180 microns). A representative portion of each sample was pulverised to < 64 µm, using a planetary Agate Ball Mill (Fig. 4) for a duration of 120 seconds. Subsequently, a well homogenised sample was placed into a sample cup with a thin mylar film at the base. As during the sampling process, a fresh pair of gloves was used for handling each new sample to avoid contamination. Geochemical analysis was carried out by a handheld Thermo Scientific Niton Energy Dispersive XRF (Niton XL3t GOLDD) spectrometer at the GSN laboratory in 2018. Each sample was analysed by placing the sample cup on the stage of the ED-XRF, which was run for 150 seconds (Fig. 4). Detection limits are shown in Fig. 5.

Figure 4. Sample preparation in an Agate Ball Mill (left) and analysis by Niton ED-XRF (right)
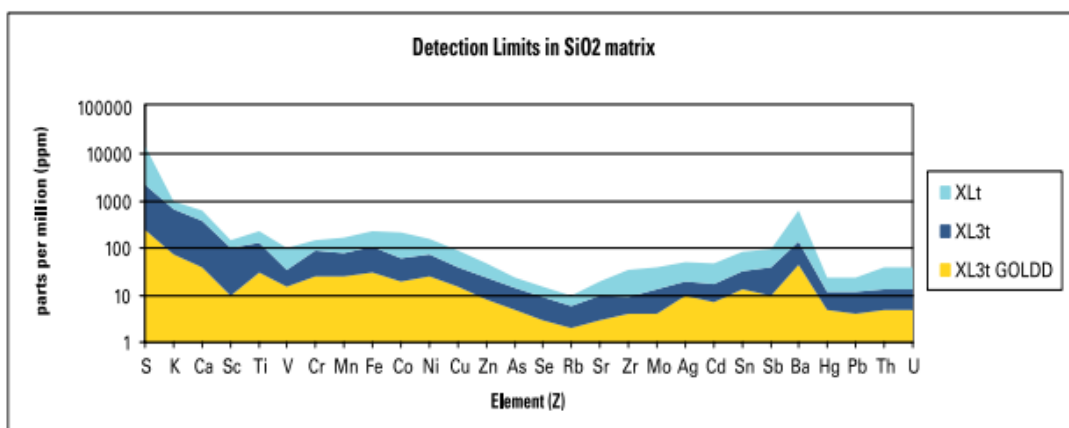

Figure 5. Detection limits of the XL3t GOLDD as compared to other models

Quality Control

The RGSP is supported by several internationally recognised Certified Reference Materials (CRMs) acquired from various institutions, i. e. Chinese manufactured standards (NCS DC 77301-3) for soil samples and Canadian originated standards (STSD_1-4) for stream sediments. Furthermore, two locally developed standards, SSTD-1 and a blank standard containing pure quartz, were used as part of the QC protocol. Duplicate and CRM samples were routinely inserted into the batches after every twentieth sample. Various QC plots of Standards and CRMs were created in Microsoft Excel to test for accuracy and precision of the analytical data (Fig. 6). In addition, evaluation of CRMs, blanks and local standards was carried out through Shewatt control charts (Piercey, 2014) and XY plots.
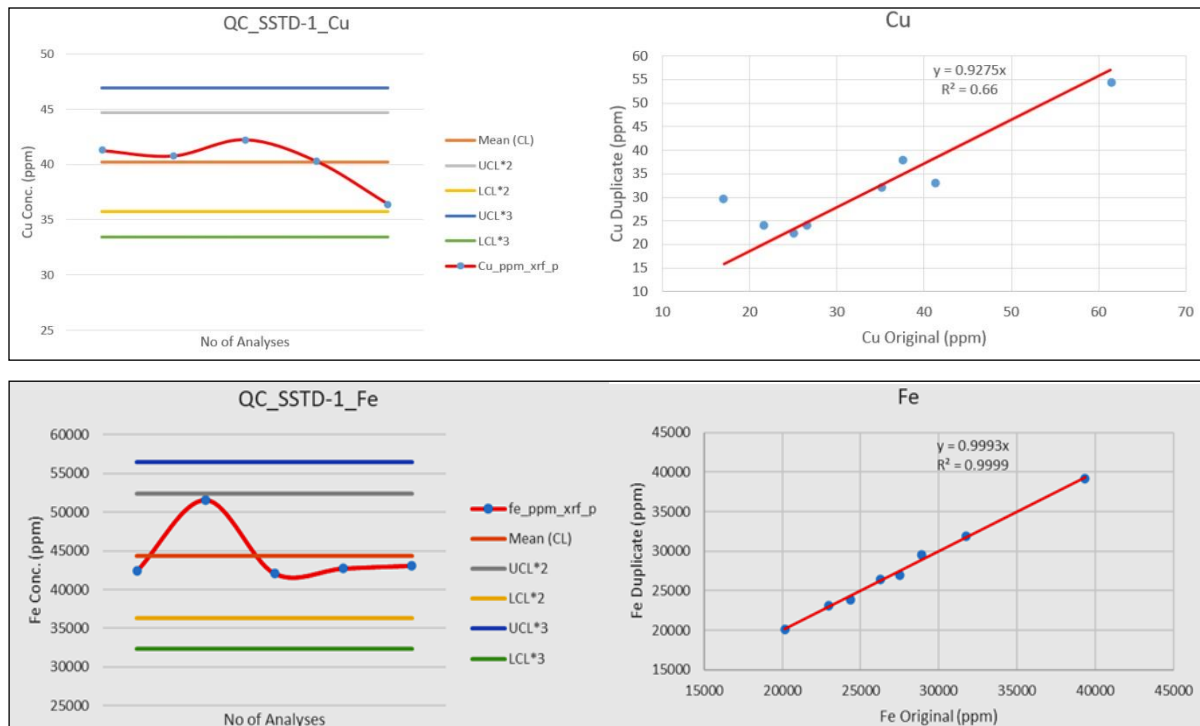
Figure 6. Control charts for copper and iron using the SSTD-1 standard to check accuracy (left); XY plot using duplicate samples for testing precision (right)

Data Visualisation

To visualise the results, basic exploratory analysis methods provided by ESRI ArcGIS software were used. To evaluate distribution trends in the data (e. g. normal, unimodal or bimodal distribution), both histograms (Figs 9, 11, 13, 15) and quantile-quantile plots (Fig. 7) were employed. Since geochemical data hardly ever show a normal distribution, the data were normalised using a logarithmic transformation before a spatial visualisation of distribution patterns was attempted. Following transformation, graduated symbol and gridded maps were produced to show the distribution of copper and iron within the survey area, the latter based on the inverse distance weighting technique (Figs 8 to 15).

Spatial Distribution of Copper

General

Copper (Cu) has an atomic number of 29, an atomic mass of 63 and two main oxidation states, i. e. +1 and +2. It has two naturally occurring isotopes ([63]Cu and [65]Cu), with relative abundances of 69.17% and 30.83%, respectively (Albanese *et al*., 2015; Salminen, 2005). Copper forms sulfide minerals such as chalcopyrite ($CuFeS_2$) and Covellite (CuS) under reducing conditions, hydroxides and carbonate minerals, such as malachite [$Cu_2CO_3 (OH)_2$)] under oxidising conditions, and can also occur in its native/metallic state as copper nuggets (Albanese *et al*., 2015; Salminen, 2005; Koljonen, 1992). Copper occurrences, many of which have been mined on a larger or smaller scale, are widespread throughout Namibia and present in almost all major lithostratigraphic units.

Copper has a higher affinity for mafic (40–60 ppm) and ultramafic rocks (40 ppm); in intermediate (20 ppm) and granitic rocks (12 ppm) it is found more rarely (Wedepohl, 1978). Black shales contain ~50 ppm Cu (Albanese *et al*., 2015; Reimann and De Caritat, 1998; Salminen, 2005), while quartzo-feldspathic and carbonate rocks contain only 5–15 ppm (Albanese *et al*., 2015; Salminen, 2005). The

average concentration of copper in the earth's crust is 68 ppm (Salminen, 2005), while the average concentration in world soils ranges from 13 to 30 ppm (Adriano, 2001; Salminen, 2005). Copper is an essential nutrient for plant and an-

imal growth at concentration levels of 5 to 30 ppm (Adrees *et al*., 2015) and 15 to 60 ppm (Koljonen, 1992), respectively. Less may lead to deficiency symptoms, whereas higher concentrations result in toxicity.
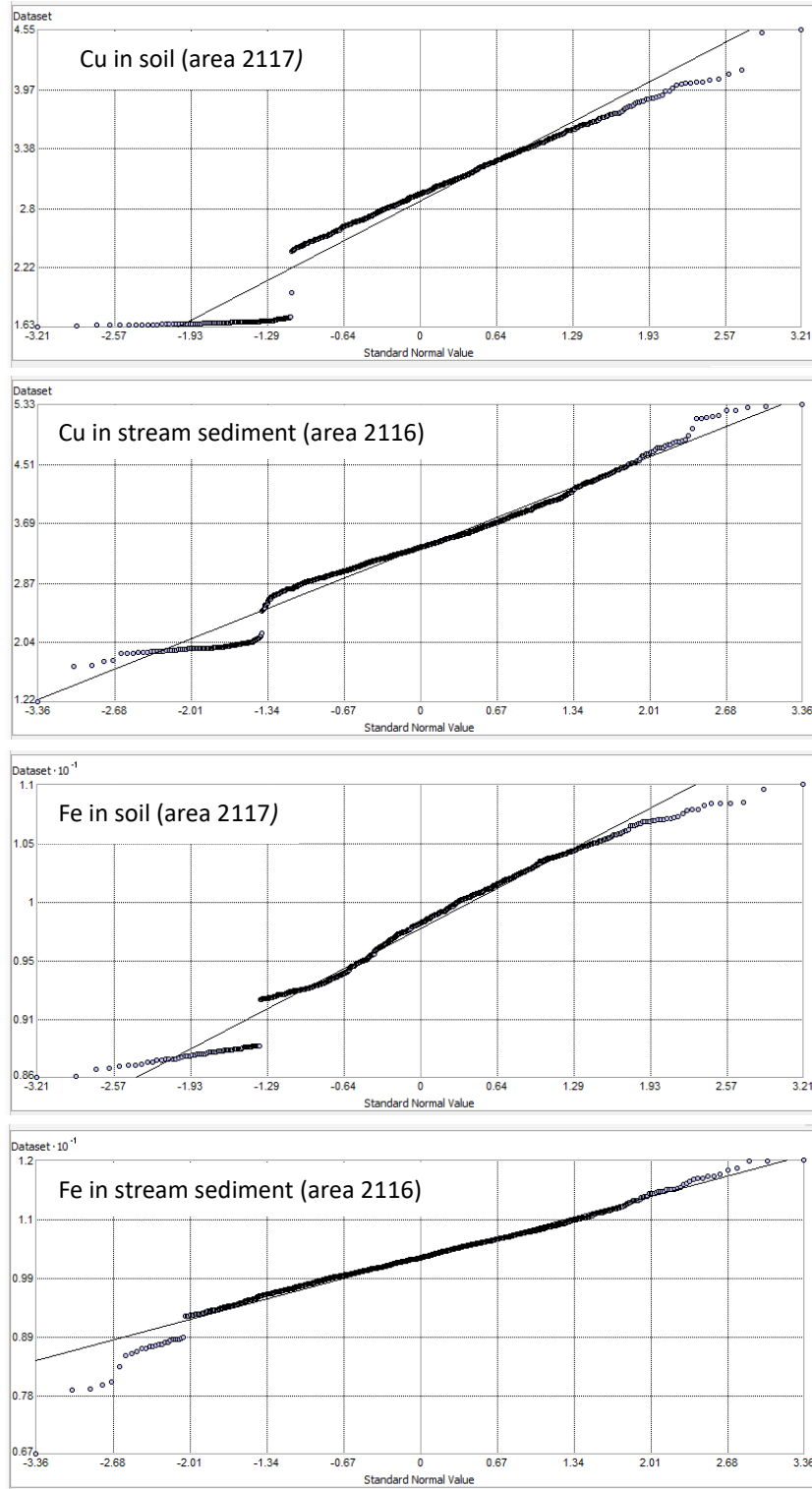

Figure 7. Normal Q-Q plots showing distribution trends in the various data sets: Cu in soil (Figs 8, 9); Cu in stream sediment (Figs 10, 11); Fe in soil (Figs 12,13); Fe in stream sediment (Figs 14,15)

Copper in soil (eastern map sheet; Area 2117)

The spatial distribution of copper in soils depends on climatic, geological and structural factors, as well as anthropogenic activities (Ballabio *et al*., 2018). In the eastern part of the Okahandja map sheet, analysed copper in soil values range from 5 to 91 ppm, with an average of 21 ppm, and a median of 19 ppm, which is comparable to average crustal values reported by Koljonen (1992) and Adriano (2001).

The area is largely covered by surficial sediments (sand, gravel, calcrete), interspersed with isolated outcrops of Damara-age metasediments (mica schist, marble, quartzite) and intrusives (pegmatite, granite, amphibolite); even more rarely high-grade metamorphic rocks of the Abbabis Complex, which forms the oldest stratigraphic unit in the area, are exposed.

The spatial distribution of copper is generally low, but variable across area 2117 (Figs 8, 9). Highest values occur in the south-east, where amphibolites and quartzo-feld-pathic gneisses of the Ekuja Basement Dome (Abbabis Metamorphic Complex) outcrop in the vicinity of the Omitiomire copper occurrence (Kitt *et al*., 2016), and around the Onjona-Eleksie Nappe Complex, consisting of paragneiss, quartzite and minor amphibolite. Younger Damara-age amphibolites intrusive into Kuiseb Formation mica schists south of the nappe complex also are likely sources of copper.

Copper in soil values decrease towards the north, concomitant with an increase of Kalahari cover over bedrock. Concentrations between 18 and 40 ppm occur in areas underlain by Damara metasediments; lowest values of less than 16 ppm are recorded in the north, where the thickness of the Kalahari overburden locally reaches 80 m, thus reducing the likelihood of geochemical bedrock anomalies finding expression in surface samples.

Copper in stream sediments (western map sheet; Area 2116)

The spatial distribution of copper in the western part of the map, where only stream sediment samples are considered in our analysis, is generally higher, averaging 34 ppm (4.5 – 197 ppm). Contrary to the comparatively low copper contents of granitic rocks postulated by Wedepohl (1978), elevated values are observed in samples representing drainages underlain by Damara-age granitoids, specifically the porphyritic Salem biotite granite, which dominates the southern part of the area, with smaller outcrops to the north-west (Figs 10, 11). Above-average concentrations also occur where hills and ranges formed by dolerite intrusions rise several hundred metres above the surrounding plains, which are underlain by deeply weathered Damara granite. Lowest values are measured in the north-east, where the Neoproterozoic Damara rocks are overlain by a thick cover of Karoo and Kalahari sediments.

Spatial Distribution of Iron

General

Iron (Fe; element 26 in the periodic table) has a molecular weight of 55.847, a melting point of 1535°C, a boiling point of 2800°C, and a specific gravity of 7.874. Four stable isotopes are found in nature: ^{54}Fe, ^{56}Fe, ^{57}Fe and ^{58}Fe. Iron commonly exists in one of three oxidation states: Fe^0 (elemental iron), Fe^{2+} (ferrous iron) and Fe^{3+} (ferric iron). It is the fourth most abundant element in the earth's crust after oxygen, silicon and aluminium, and accounts for over 5% of the crust's mass. Its average crustal abundance is 7% (Williamson, 1998), while the W.H.O. maximum allowable limit for iron is 5% (Ogunlana *et al*., 2020). Iron is an essential element for almost all living organisms as it drives metabolic processes, including oxygen transport, DNA synthesis and photosynthesis in plants. If the concentration of available (soluble) iron, which is only a small fraction of the total Fe content in soils and stream sediments, is less than 50 ppm, deficiency symptoms result, while toxic effects may be observed where it exceeds 500 ppm. Iron is present in primary minerals, in the crystal lattices of clays and in weathered soils. An important feature of iron is its ability to combine with other metals to form a variety of alloys for a host of different uses and applications.
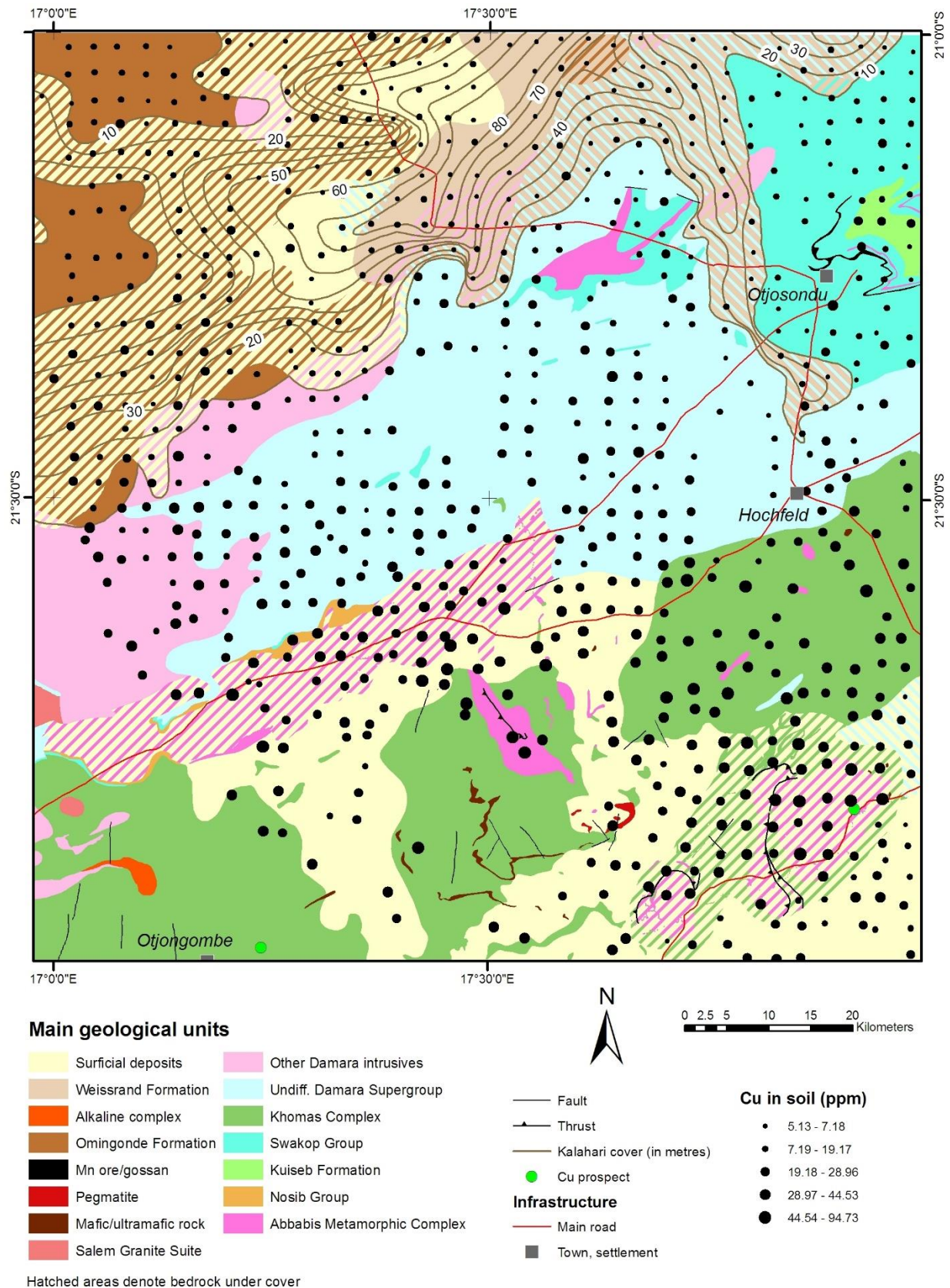
Figure 8. Graduated symbol visualisation displaying copper in soil concentrations in the eastern half of the Okahandja map sheet (area 2117), superimposed on a simplified geological map showing main lithological units, structures and copper prospects
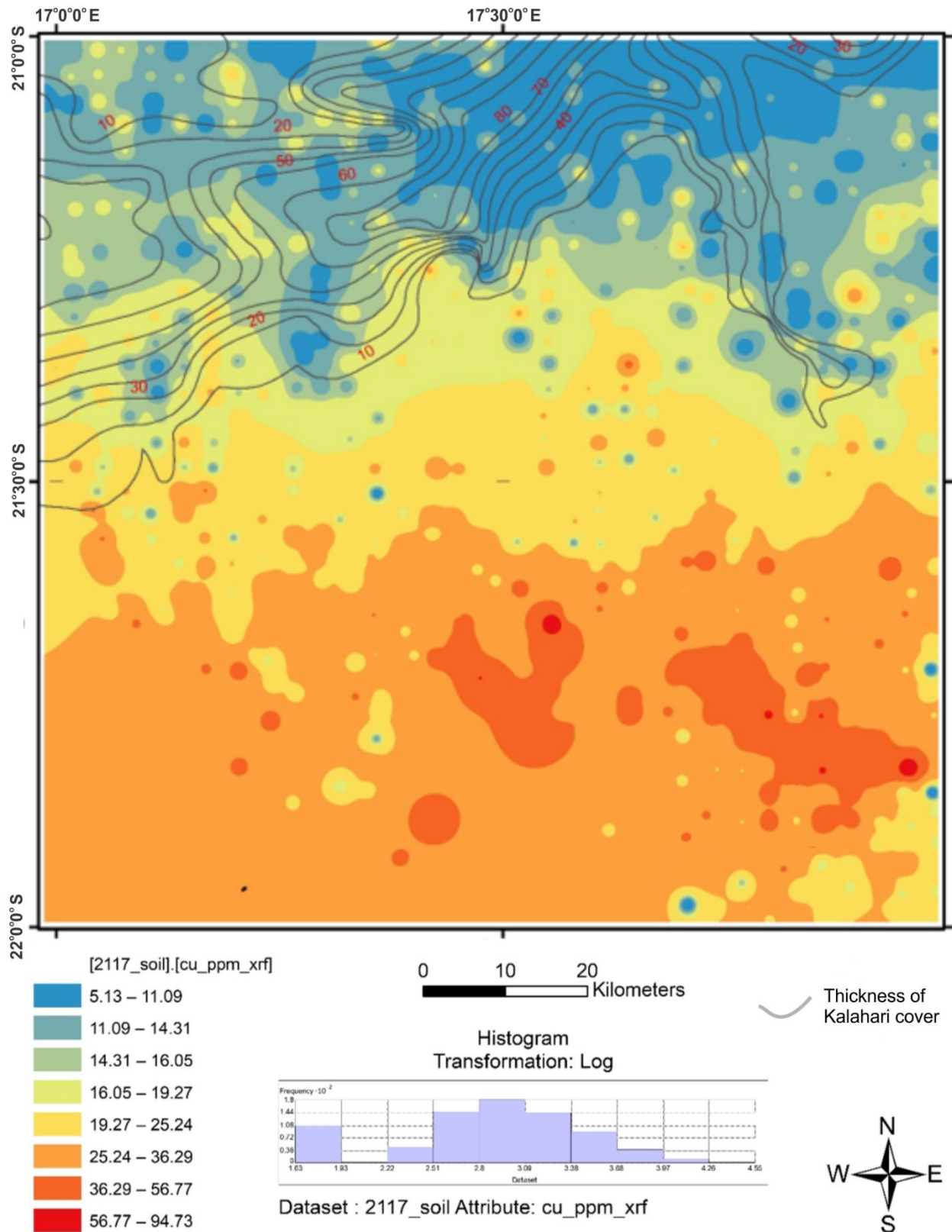
Figure 9. Gridded map of copper in soil concentrations based on inverse distance weighting (IDW) in the eastern half of the Okahandja map sheet (area 2117), showing a marked north-south trend; the histogram gives the distribution of abundances.
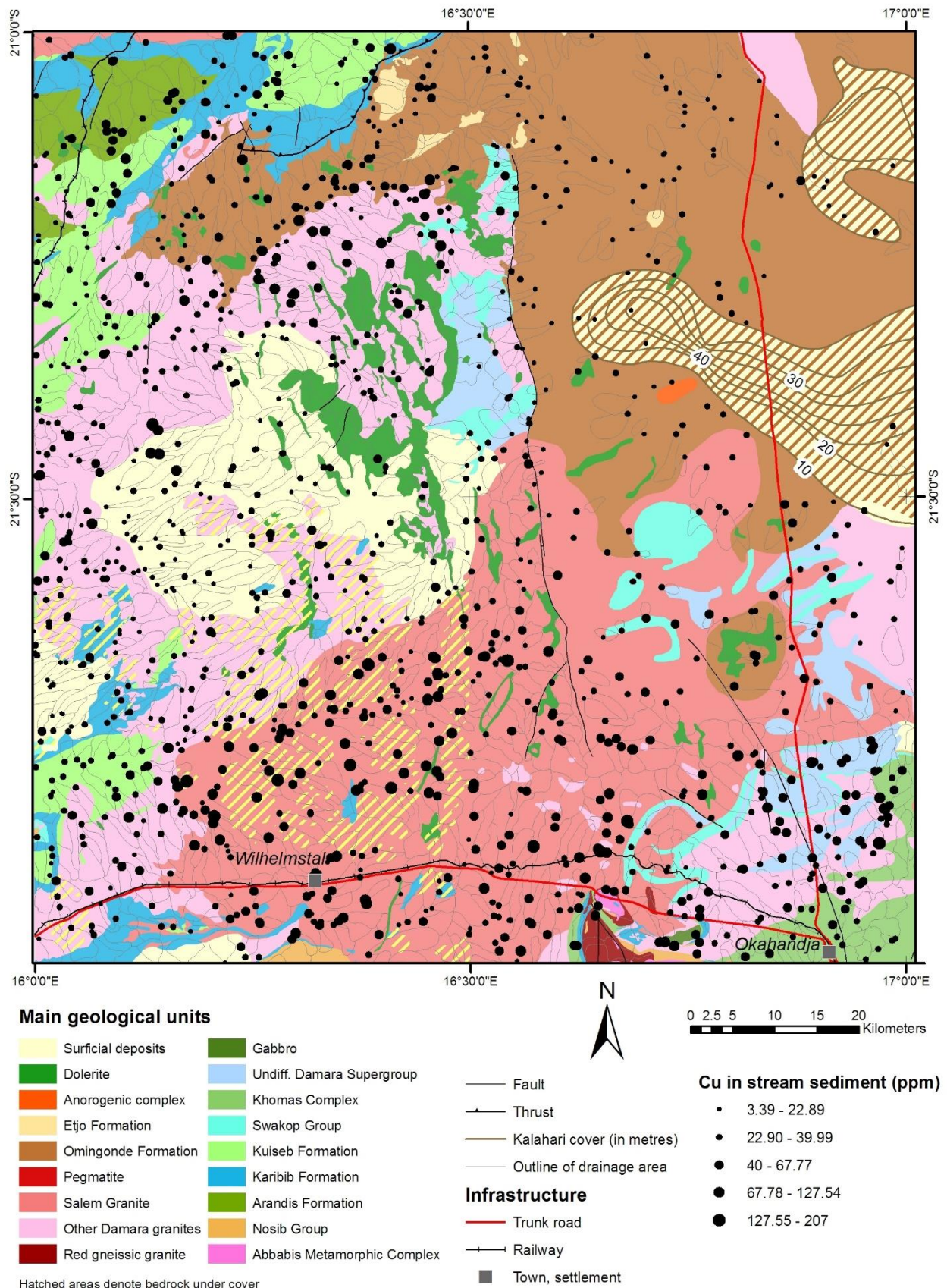
Figure 10. Graduated symbol visualisation displaying copper in stream sediment concentrations in the western half of the Okahandja map sheet (area 2116), superimposed on the simplified geological map showing main lithological units and structures
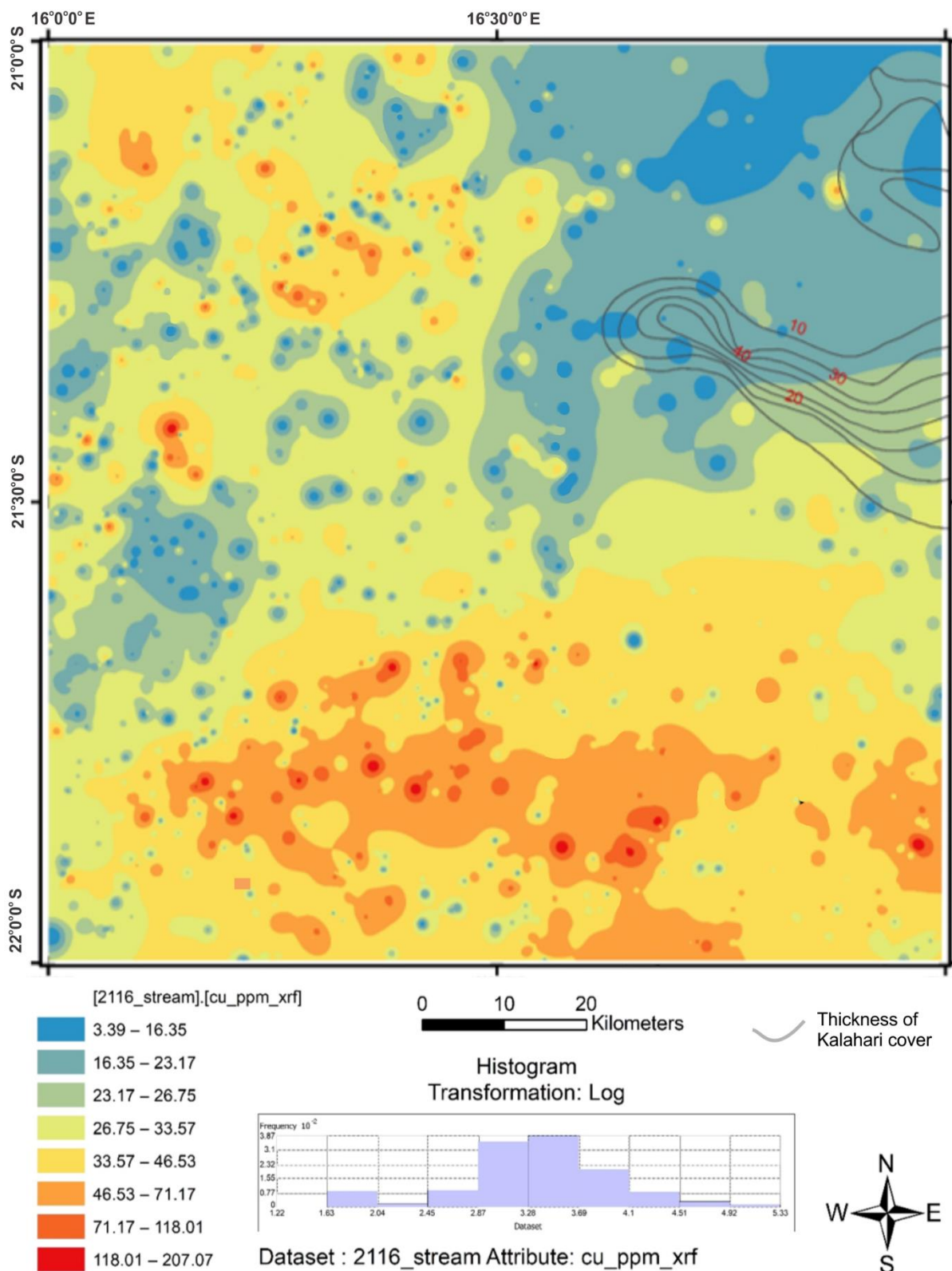
Figure 11. Gridded map showing copper in stream sediment concentrations based on inverse distance weighting (IDW) in the western half of the Okahandja map sheet (area 2116); the histogram gives the distribution of abundances.

Iron in soil (eastern map sheet; Area 2117)

In the eastern half of the area, Fe concentrations in soil samples range from 5286 ppm (0.53%) to 58216 ppm (5.82%), with an average of ~2%. This figure is below the documented Fe concentration in both the upper continental crust (3.3 %) and in world soils (3.5%; Koljonen, 1992).

The highest values of >33500 ppm are encountered in the southern central part (Figs 12, 13), which is underlain by mica schists and marbles of the upper Swakop Group (Damara Supergroup), intruded locally by amphibolites and pegmatites. Basement gneisses of the Abbabis Metamorphic Complex seem to have yielded somewhat lower Fe concentrations to the soil during weathering (~26000 to 33500 ppm; SE corner of the area). As with copper, iron concentrations drop steadily towards the north, which may be attributed to the increasing Cenozoic overburden, consisting of unconsolidated to semi-consolidated sediments of the Kalahari Group and Karoo-age mudstones and sandstones, evidently low in the two elements under consideration.

Iron in stream sediments (western map sheet; Area 2116)

Measured iron concentrations in stream sediments of the western part of the map sheet range from 851 ppm to the 169800 ppm (or 16.98 %), with an average concentration of 3.4%, which is higher than the respective average in soil samples in the east (2%), and close to the upper continental crust average of 3.3%. The overall distribution pattern is similar to that of copper in the same area, with highest concentrations occurring in the south and northwest (Figs 14, 15).

Samples representing catchments underlain by granitic rocks, specifically the biotite (Fe, Mg phyllosilicate) – rich granitoids of the Salem Suite, tend to show greater concentrations than those deriving from drainages dominated by metasedimentary rocks. Once again lowest values are observed in areas of thick Karoo and/or Kalahari cover in the northeast.

Summary and conclusions

This report presents generalised spatial distribution maps of copper and iron within area 2116 Okahandja. On account of local topography only stream sediment samples were considered in the western part (area 2116), while in the largely sand-covered eastern portion (area 2117) only soil samples were used. In the latter area, copper and iron in soil show much lower absolute and average values than the stream sediment samples in the west, which represent drainages of hilly areas with rock outcrops. In the east highest concentrations occur in the vicinity of scarce basement outcrops (Abbabis Metamorphic Complex), while in the west, areas underlain by granitic or mafic intrusives show elevated values. The distinct N-S trend in both copper and iron concentrations in area 2117 may be jointly ascribed to bedrock composition and Kalahari overburden, which increases in a northerly direction (Figs 9, 13). Apart from the rock types outcropping in or underlying the sampled area and thickness of Kalahari/Karoo cover, anthropogenic activities in this agricultural region may account for local highs, although care was taken to collect samples away from roads and fences, and other possible sources of contamination. Potentially toxic copper concentrations in stream sediments were measured north of the main road and railway between Okahandja and Wilhelmstal (Fig. 10), possibly due to polluting effects.

Analytical results were also compared to known crustal abundances. This showed copper and iron in soil samples of area 2117 on average to be lower than the documented values for upper continental crust and world soils, while concentrations of the same elements in the west, where stream sediments were analysed, are within small margins of the above values.

This case study shows that pXRF analysis, while having relatively high lower limits of detection (Fig. 5) compared to conventional analytical methods (XRF/ICP), provides a fairly reliable picture at regional scale of the distribution of comparatively abundant elements, such as Fe and Cu. However, it is unsuitable for elements of low abundance (e. g. gold) because of too high lower limits of detection.
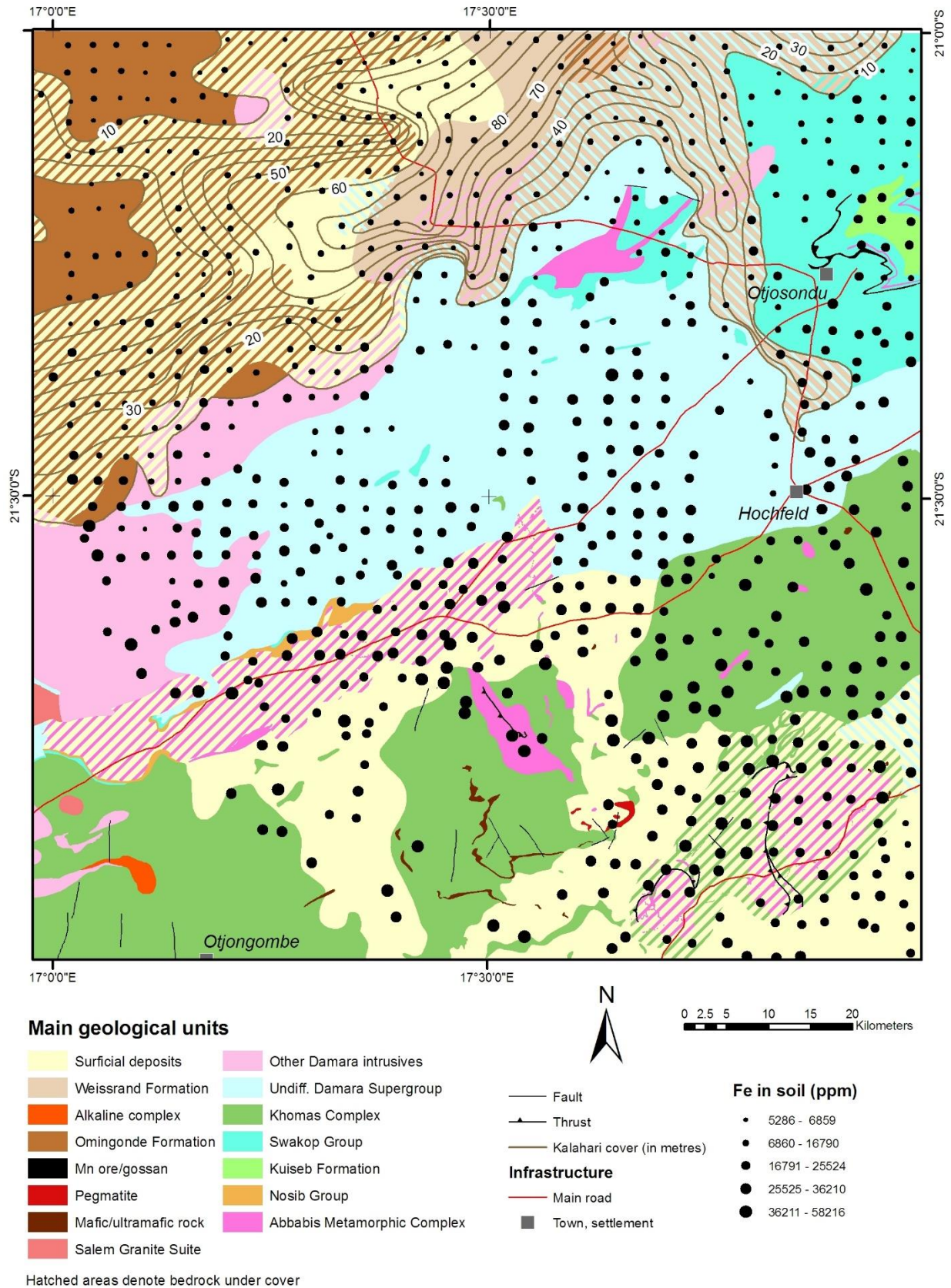
Main geological units

Surficial deposits	Other Damara intrusives		
Weissrand Formation	Undiff. Damara Supergroup		
Alkaline complex	Khomas Complex		
Omingonde Formation	Swakop Group		
Mn ore/gossan	Kuiseb Formation		
Pegmatite	Nosib Group		
Mafic/ultramafic rock	Abbabis Metamorphic Complex		
Salem Granite Suite			

Fault
Thrust
Kalahari cover (in metres)

Infrastructure
Main road
Town, settlement

Fe in soil (ppm)
5286 - 6859
6860 - 16790
16791 - 25524
25525 - 36210
36211 - 58216

Hatched areas denote bedrock under cover

Figure 12. Graduated symbol visualisation displaying iron in soil concentrations in the eastern half of the Okahandja map sheet (area 2117), superimposed on the simplified geological map showing main lithological units and structures
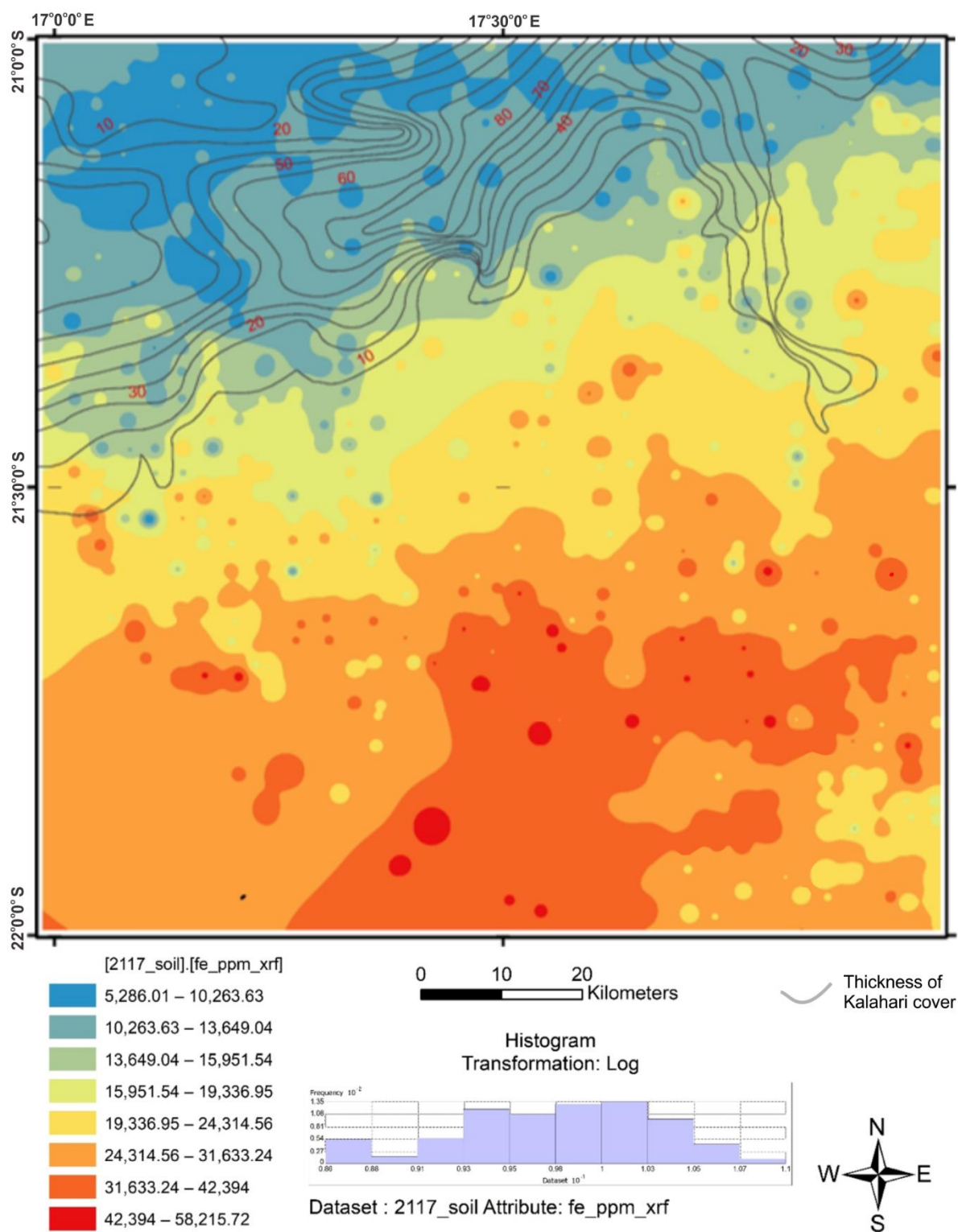
46

Figure 13. Gridded map showing iron in soil distribution based on inverse distance weighting (IDW) in the eastern half of the Okahandja map sheet (area 2117), showing a marked north-south trend; the histogram gives the distribution of abundances.
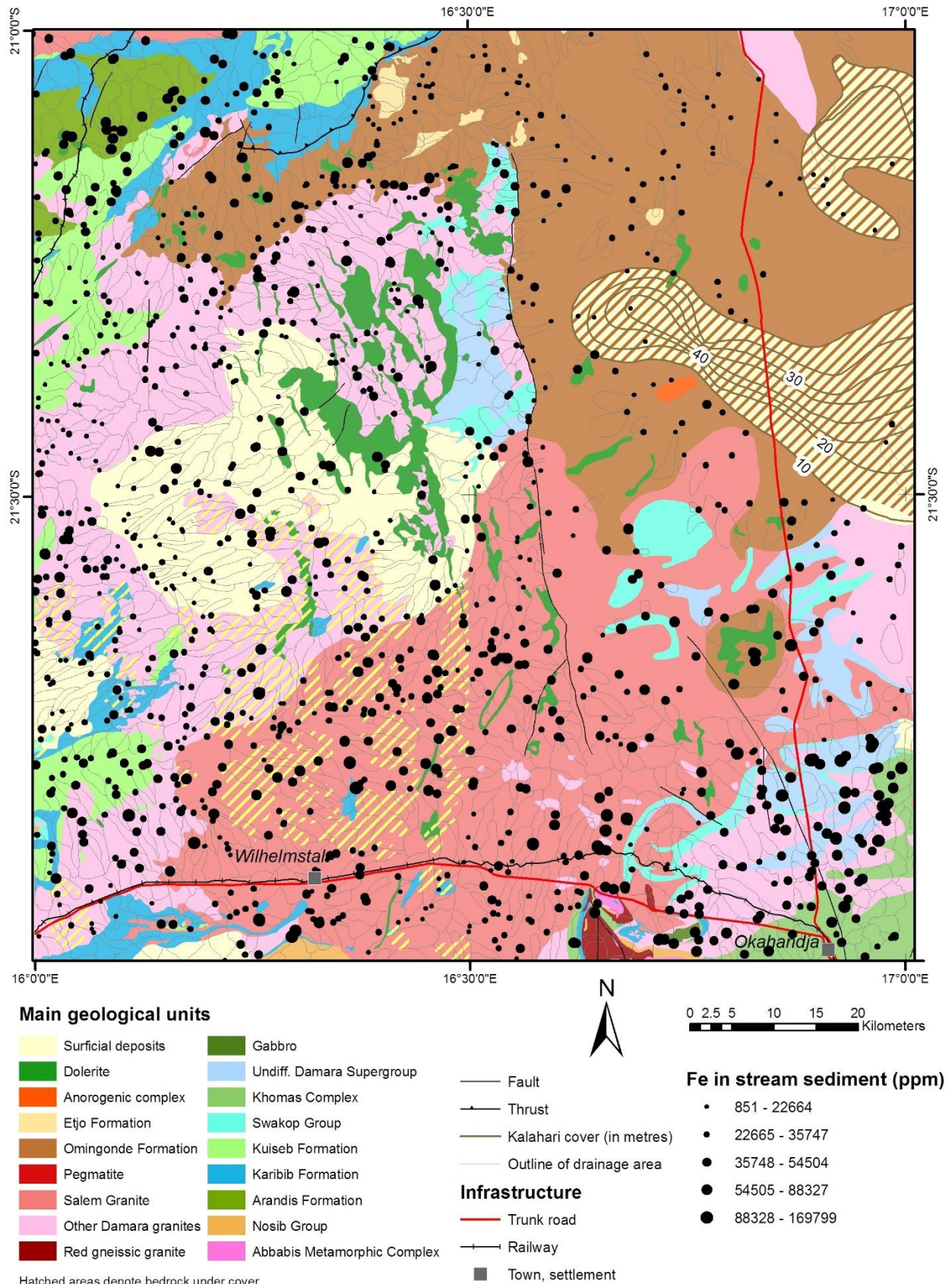
Figure 14. Graduated symbol visualisation displaying iron in stream sediment concentration in the western half of the Okahandja map sheet (area 2116), superimposed on the simplified geological map showing main lithological units and structures
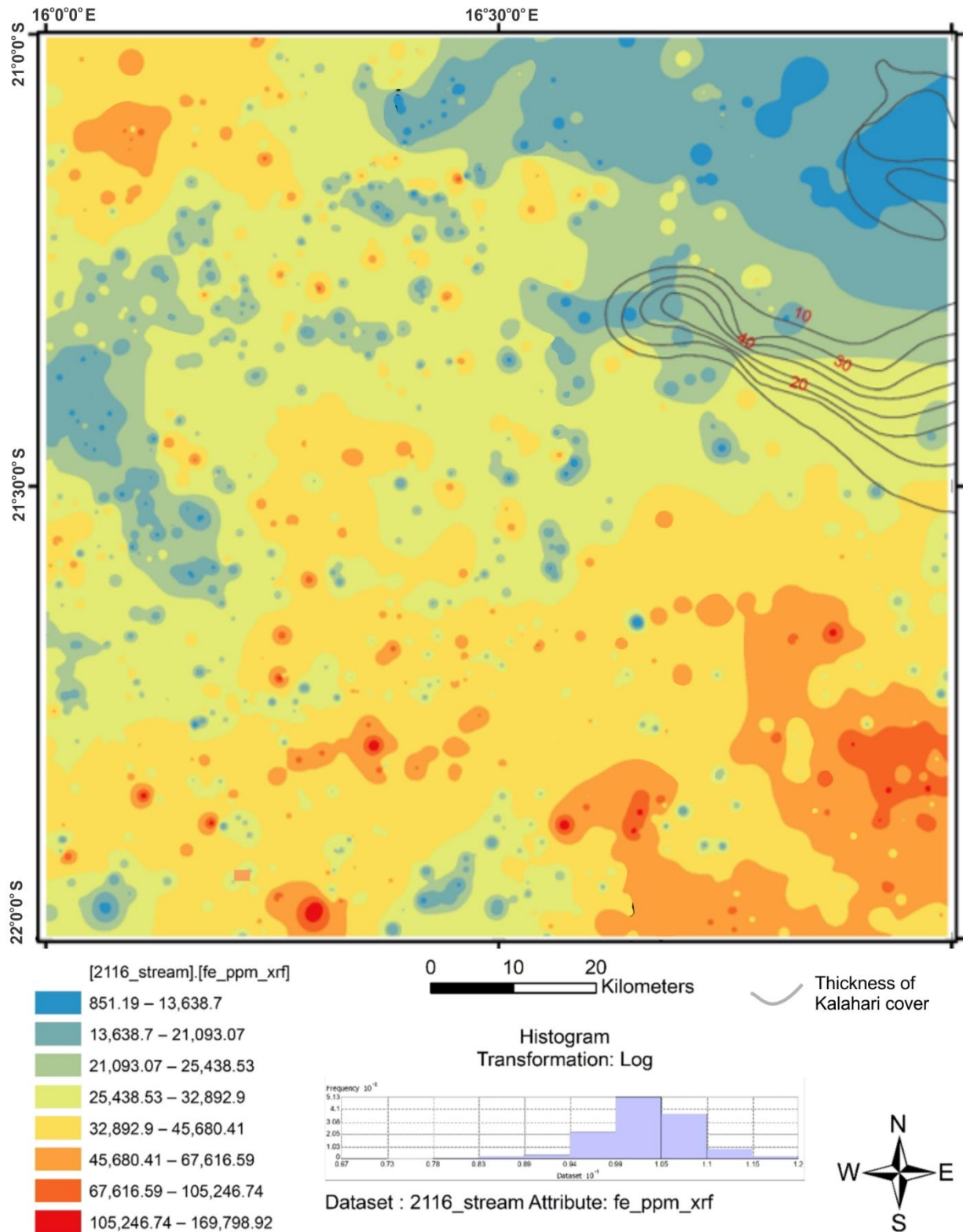
Figure 15. Gridded map showing the distribution of iron in stream sediment based on inverse distance weighting (IDW) in the western half of the Okahandja map sheet (area 2116); the histogram gives the distribution of abundances.

With regard to the chosen visualisation methods, graduated symbols showing relative abundance of the analysed elements (Figs 8, 10, 12, 14) realistically reflect anomalous values in relation to the underlying geology, which can be explored in more detail by mineral exploration companies, land use planers, health authorities and other stakeholders. An even clearer picture of overall element distribution is provided by gridded maps, based on statistical methods (Figs 9, 11, 13, 15), in areas of high sample density; however, such interpolations have to be used with caution where samples are few and far between, as in the south-west of area 2117 (Fig. 2). Here, meaningful interpretive results can only be obtained from the stream sediment samples dominating this sector, rather than the few scattered soil samples.

References

Adrees, M., Ali, S., Rizwan, M., Ibrahim, M., Abbas, F., Farid, M. and Bharwana, S. A. 2015. The effect of exess copper on growth and physiology of important food crops: a review. *Environmental Science and Pollution Research*, **22**, 8148 - 8162.

Adriano, D. C. 2001. Trace elements in terrestrial environments. Biogeochemistry, Bioavailability, and Risks of Metals, 2nd ed. Springer, New York, 867 pp.

Albanese, S., Sadeghi, M., Lima, A., Cicchella, D., Dinelli, E. and Valera, P. 2015. GEMAS: Cobalt, Cr, Cu, Ni distribution in agricultural and grazing land soil of Europe. *Journal of Geochemical Exploration*, **154**, 81-93.

Ballabio, C., Panagos, P., Lugato, E., Huang, J., Orgiazzi, A., Jones, A. and Montanarella, L. 2018. Copper distribution in European topsoils: An assessment based on LUCAS soil survey. *Science of the Total Environment*, **636**, 282 -298.

Kitt, S., Kisters, A., Steven, N., Maiden, K. and Hartmann, K. 2016. Shear-zone hosted copper mineralisation of the Omitiomire deposit - Structural controls of fluid flow and mineralisation during subduction accretion in the Pan-African Damara Belt of Namibia. *Ore Geology Reviews*, **75**, 1 - 15.

Koljonen, T. 1992. *The Geochemical Atlas of Finland, Part 2: Till*. Geological Survey of Finland, Espoo, 218 pp.

Linus, J. and Schreiber, U. 2017. *The Geology of Area 2116 Okahandja*. Explanation of sheet 2116, scale 1:250 000. Geological Survey of Namibia, Ministry of Mines and Energy, Windhoek (unpubl.), 31 pp.

Ogunlana, R., Korode, A. and Ajibade, Z. 2020. Assessing the level of heavy metals concentration in soil around transformer at Akoko community of Ondo State, Nigeria. *Journal of Applied Sciences and Environmental Management*, **24(12)**, 2183-2189.

Piercey, S. J. 2014. Modern Analytical Facilities 2. A Review of Quality Assurance and Quality Control (QA/QC) Procedures for Lithogeo-chemical Data. *Geoscience Canada,* **41(1**), 75–88.

Reimann, C. and De Caritat, P. 1998. *Chemical elements in the environment.* Springer, Berlin, 407 pp.

Salminen, R. 2005. *Geochemical Atlas of Europe. Part 1: Background Information, Methodology and Maps*. Geological Survey of Finland, Espoo, 526 pp.

Tewari, R. 2003. The origins of iron working in India: new evidence from the Central Ganga Plain and the Eastern Vindhyas. *Antiquity*, **77(297)**, 536-544. https://doi:10.1017/ S0003598X00092590

Wedepohl, K. H. 1978. *Handbook of Geochemistry*, Vol. 2, Part 5. Springer, Berlin-Heidelberg-New York, 1578 pp, 266 figs, 576 tables.

Williamson, M. A. 1998. Iron. *In: Geochemistry. Encyclopedia of Earth Science*. Springer, Dordrecht, The Netherlands. https:// doi.org/10.1007/1-4020-4496-8_172